IEEE Access
Multidisciplinary | Rapid Review | Open Access Journal

Received April 11, 2021, accepted April 20, 2021, date of publication April 22, 2021, date of current version May 3, 2021.

Digital Object Identifier 10.1109/ACCESS.2021.3075072

Methodology for Security Analysis of Grid-Connected Electric Vehicle Charging Station With Wind Generating Resources

GYEONGMIN KIM, (Student Member, IEEE), AND JIN HUR, (Senior Member, IEEE)
Department of Climate and Energy Systems Engineering, Ewha Womans University, Seoul 03760, Republic of Korea
Corresponding author: Jin Hur (jhur@ewha.ac.kr)

This work was supported by the Korea Electric Power Corporation under Grant R18XA06-55.

ABSTRACT The project Carbon-Free Island Jeju by 2030 promoted by the Republic of Korea aims to expand the renewable energy sources centered on wind power in Jeju Island and supply electric vehicles for eco-friendly mobility. However, the increased penetration rate of electric vehicles and expansion of variable renewable energy sources can accelerate the power demand and uncertainty in the power generation output. In this paper, power system analysis is performed through electric vehicle charging demand and wind power outputs prediction, and an electric vehicle charging decentralization algorithm is proposed to mitigate system congestion. In order to predict electric vehicle charging demand, the measurement data were analyzed, and random sampling was performed by applying the weight of charging frequency for each season and time. In addition, wind power outputs prediction was performed using the ARIMAX model. Input variables are wind power measurement data and additional explanatory variables (wind speed). Wind power outputs prediction error (absolute average error) is about 9.6%, which means that the prediction accuracy of the proposed algorithm is high. A practical power system analysis was performed for the scenario in which electric vehicle charging is expected to be higher than the wind power generation due to the concentration of electric vehicle charging. The proposed algorithm can be used to analyze power system problems that may occur due to the concentration of electric vehicle charging demand in the future, and to prepare a method for decentralizing electric vehicle charging demand to establish a stable power system operation plan.

INDEX TERMS Electric vehicle, charging station, wind generating resources, charging demand, wind power forecasting, security analysis.

I. INTRODUCTION

The United Nations Framework Convention on Climate Change (UNFCCC) aims to reduce global warming caused by greenhouse gases (GHGs), such as carbon dioxide. To reduce GHG emissions, several countries are increasing the proportion of renewable and clean sources, such as wind and solar powers, in energy generation to minimize the existing fossil fuel-based power generation [1]–[3]. Additionally, eco-friendly mobility (e.g., electric vehicles (EVs) and hydrogen vehicles) and improvement of related infrastructure are being promoted to reduce the use of carbon in the transportation sector. The large-scale penetration of renewable energy and expansion of EV supply will affect the operation of future power systems significantly. The establishment of a flexible and decentralized power system operational plan that accounts for renewable energy generation output and EV charging demand is essential [4], [5]. The Republic of Korea aims to expand the supply of renewable energy and eco-friendly mobility through various projects, such as the Korean version of the Green New Deal [6], [7], Renewable Energy 3020 Implementation Plan [8], and Carbon-Free Island Jeju by 2030 [9]. Particularly, the Carbon-Free Island Jeju by 2030 project is leading the supply of renewable energy in Korea that comprises a 4,085 MW of renewable energy generation facilities. They intend to supply 100% of the electricity demand in the province as a renewable energy source to replace 3,770,000 vehicles with EVs.

The progress in EV supply generates large-scale power demand in terms of EV charging, and if EVs are penetrated to the grid, which can affect the power system adversely through an increase in the peak load or causing a line overload [10].

The associate editor coordinating the review of this manuscript and approving it for publication was Zhiyi Li.

To improve these limitations, grid expansion or new component is required. However, since this method is not economically feasible, a Vehicle to Grid (V2G) study was conducted to design a charger in a way that enables bidirectional power flow between the system and the Energy Storage System (ESS) [11]. Additionally, the existing fossil fuel and nuclear power system operations utilize dispatchable energy sources that can be dispatched on demand. If an imbalance occurs in the power supply and demand, a controllable power generation facility is used to reinstate balance. However, renewable energy sources have large variability and uncertainty due to reliance on meteorological variables, such as solar irradiance, wind speed, and wind direction. As the proportion of renewable energy generation facilities penetrating the power system increases, output variability is expected to occur in both demand and supply. A large-scale transmission and substation investment plan must be established based on the evaluation of power system stability, considering the uncertainty of the system element and the stability of renewable energy as a power source. Therefore, prediction modeling of the renewable energy generation output is essential to establish a charge distribution plan through EV charging demand prediction. Moreover, the uncertainty of the grid connection owing to the intermittency and output constraints of variable renewable energy sources must be controlled [12]. There exist many literatures that are focusing on EVs charging station integration with wind power penetration, energy management for intelligent secured framework considering EVs [13]–[15]. The previous study [15] designed the optimal charging facility for EV charging station. For optimization of the proposed algorithm, variables such as charging time of EVs, charging station capacity and harvested power from wind energy are used. The seasonal power profile of wind turbine was calculated and used for optimization, but it is difficult to know how the wind power output was predicted because the profile process was not clearly described. In this paper, wind power outputs prediction was performed using the ARIMAX model, and the error of the prediction algorithm was analyzed through comparison with measured data. It can be seen that wind power generation prediction was performed more clearly than previous studies. In the previous study [16], the average charging demand for one EV was calculated and the EVs charging demand was estimated by using data on the number of future EVs and the average mileage per vehicle. The average mileage per vehicle is the calculated mileage based on the number of gasoline vehicles and gasoline consumption. Therefore, this is calculated without considering the characteristics of EVs such as charging time and frequency, so the data for EV charging demand prediction may be distorted. In this paper, the EV charging demand was predicted by analyzing the charging frequency and demand (in MW) for each time period considering the start and end times of charging in all charging data along with the charging time and demand of EVs. The annual EV charging demand was predicted for the year 2030 based on the number of EVs supplied in 2018. The main contribution of this study can be summarized as follows:

- Improved EV charging data analysis than previous studies: fitting the charging frequency and demand curve for each time period, and predicting EV charging demand considering charging frequency weighting
- Through the proposed algorithm, it is possible to analyze the instability of the power system in advance due to the increase in wind power generation capacity and EV charging demand, and can be used to devise a plan to decentralize EV charging demand.
- It can be used to establish a stable power system operation plan by applying wind power output data estimated using the ARIMAX model and predicting EV charging demand to the real-time market.

This paper analyzes the effect of the increase in EV charging demand and in the proportion of wind power generation on the power system. In addition, an algorithm for predicting EV charging demand and wind power output is proposed to establish a reliable and stable power system operation plan through decentralization of EV charging demand. The correlation between the EV charging time is analyzed, charging frequency, and charging demand by season and time. Additionally, the EV charging frequency weight for each hour was calculated based on EV charging demand measured data.

The remainder of this paper is organized as follows. In Section 2, the probabilistic charging frequency data are calculated using random sampling, based on the weight calculated by analyzing the EV charging frequency to predict the EV charging demand in 2030. Section 3 presents the wind power output prediction performed using the ARIMAX model by aggregating the data of past wind speed (m/s) and measured wind power outputs in MW for each wind farm on four buses. The power output forecasting of each bus was converted to the capacity factor of the bus, and the outputs of the new wind farms scheduled to be built in Jeju Island by 2030 were predicted by utilizing the associated capacity output of each bus and the installation capacity of each new wind farm. In Section 4, we discuss the system analysis by combining the EV charging demand predicted using stochastic random sampling in Section 2 with the wind power outputs predicted using the data obtained in Section 3. Finally, Section 5 presents the conclusions.

II. PREDICTION OF ELECTRIC VEHICLE (EV) CHARGING DEMAND

As the supply of eco-friendly mobility increases to implement the carbon reduction policies, the need to analyze EV charging demand arises to serve new EV charging stations in the future. The increase in EV charging demand can affect the power system adversely by increasing the peak load or generating a line overload.

A. EV CHARGING DEMAND DATA

To predict the EV charging demand, it is necessary to analyze the measured data from EV charging stations. To analyze EV charging demand, data on the charging station names,

TABLE 1. Overview of electric vehicle charging station data.

Data	Content
Charging station location	- To map the EV charging demand data to the 154-kV bus, the distance between each charging station and bus is calculated based on the location (latitude, longitude) of the EV charging station
Charging time and charging frequency	- To analyze EV charging patterns and predict charging demand, the data of charging time and frequency of each charger were analyzed based on the season and system load criteria
Charging power (MW)	- Charging power data based on EV charging time

TABLE 2. Samples of electric vehicle charging data from Jeju island.

Charging station ID	Charging power (kW)	Charging time (min)	Charging start date	Charging end date
1	36.09	35	2018-01-01 10:34	2018-01-01 11:09
2	18.97	22	2018-01-01 15:04	2018-01-01 15:26
⋮	⋮	⋮	⋮	⋮
63	32.16	35	2018-12-31 22:59	2018-12-31 23:34
64	39.18	37	2018-12-31 23:19	2018-12-31 23:56

charging power (MW), charging time (minutes), and charge start and end date data are used. An overview of EV charging station data is shown in Table 1. Table 2 summarizes an example of EV charging data.

EV charging stations data were mapped to the Jeju system bus to evaluate the system impact caused by EV charging demand. The EV charging stations were linked to the bus based on the minimum distance calculated. Fig. 1 depicts the locations of the 154 kV buses and EV charging stations marked in blue and red, respectively.

B. EV CHARGING DEMAND AND CHARGING FREQUENCY ANALYSIS

To decentralize the EV charging demand, the EV charging data were analyzed by dividing the time zones into low,

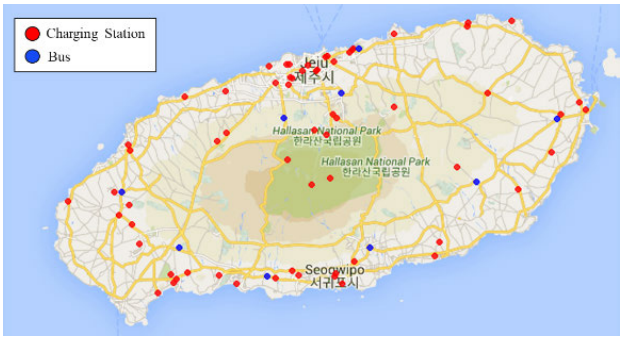

FIGURE 1. Locations of 154-kV buses and electric vehicle charging stations in Jeju Island.

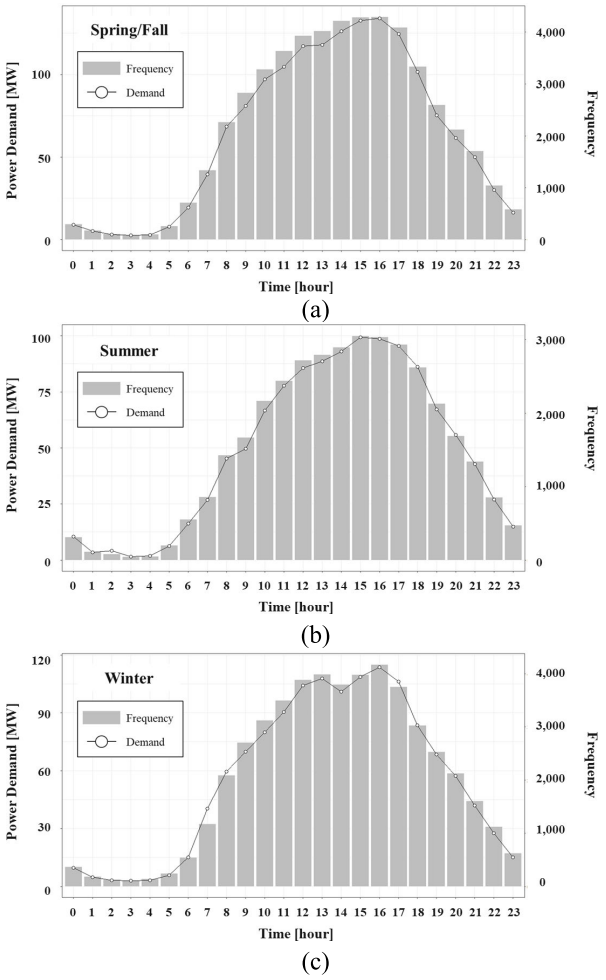

FIGURE 2. Comparison of seasonal electric vehicle charging demand and charging frequency.

intermediate, and peak loads based on the grid load classification criteria. Table 3 presents the criteria for classifying the system load times in different seasons [17].

As the Jeju island is a tourist destination, the EV charging demand pattern varies based on the season. The seasonal EV charging demand and charging frequency were analyzed based on the load time classification in Table 3, considering the number of days (153, 92, and 119 days in spring/fall, summer, and winter, respectively) in each season. Fig. 2 graphically illustrates the comparison of seasonal EV charging demand and charging frequency where it can be seen that the charging demand and frequency patterns are similar in all seasons.

Fig. 3 illustrates the results of analyzing the EV charging frequency by season based on time, considering the number of days in each season. As Jeju Island is a tourist island, EV charging frequency is high in winter and summer owing to the inflow of numerous tourists. Particularly, the EV charging frequency is high between 10:00 and 17:00 h.

Subsequently, the weights of each season and time were calculated by analyzing the EV charging demand and frequency comparisons (Fig. 2) and the seasonal EV charging

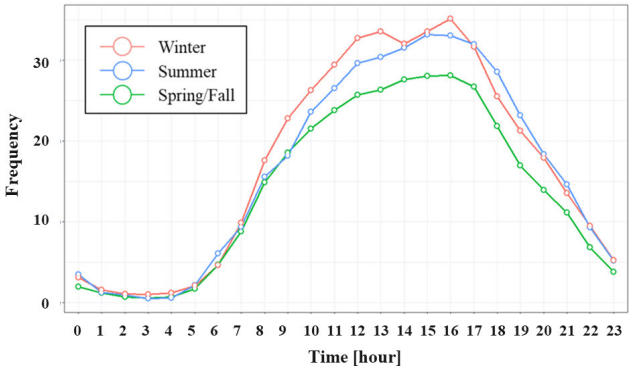

FIGURE 3. Comparison of electric vehicle charging frequency by season.

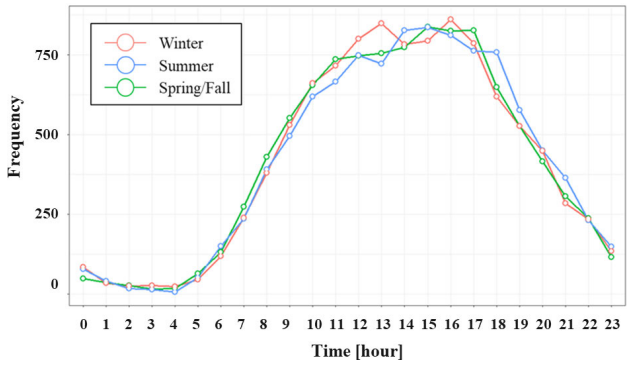

FIGURE 4. Sampling of electric vehicle charging frequency by season and time based on the weighted application.

TABLE 3. Classification of seasonal demands.

Time/ Season	Spring/Fall (March–May, September–October)	Summer (June–August)	Winter (January–February, November–December)
Low load	23:00~09:00	23:00~09:00	23:00~09:00
Intermediate load	09:00~10:00 12:00~13:00 17:00~23:00	09:00~10:00 12:00~13:00 17:00~23:00	09:00~10:00 12:00~17:00 20:00~22:00
Peak load	10:00~12:00 13:00~17:00	10:00~12:00 13:00~17:00	10:00~12:00 17:00~20:00 22:00~23:00

frequency comparisons (Fig. 3). The EV charging frequency by season and time was extracted based on the random sampling of predicted data for 2030 using the calculated weights. Fig. 4 illustrates the sampling data of the EV charging frequency by season and time considering the weight for each time period.

The extracted sampling data are applied to predict the EV charging demand for each season in 2030 in Section 2.C.

C. PREDICTION OF EV CHARGING DEMAND IN JEJU ISLAND

In this section, the EV charging demand is predicted for the year 2030 using the 2018 data of charging demand

TABLE 4. Electric vehicle charging demand for 2018 and 2030.

Category	Electric vehicle charging demand (2018)	Electric vehicle charging demand (2030)
Annual	4011.1 MW	97,253.8 MW
Spring/Fall	1686.0 MW	40,878.6 MW
Summer	1013.8 MW	24,580.6 MW
Winter	1311.3 MW	31,794.5 MW

TABLE 5. Prediction of electric vehicle charging demand for 2030.

Time/ Season	Spring/Fall (March–May, September–October)	Summer (June–August)	Winter (January–February, November–December)
Low Load	31.0 MW	30.4 MW	29.7 MW
Intermediate load	113.8 MW	117.2 MW	142.8 MW
Peak load	122.3 MW	119.6 MW	94.6 MW

and number of EVs. In 2018, the number of EVs supplied was 15,549 [18], and the charging demand for EVs was 4011.1 MW. Considering that the number of EVs is expected to be 3,770,000 [9] in 2030, the charging demand for EVs is predicted based on the number of EVs supplied and the demand for EVs in 2018. The charging demand for EVs in 2030 is predicted using (1).

$$EV\ charging\ demand_{2030} = EV\ charging\ demand_{2018} \times \frac{The\ number\ of\ EV_{2030}}{The\ number\ of\ EV_{2018}} \quad (1)$$

The predicted EV charging demand for the year 2030 is approximately 97,253.8 MW. Table 4 lists the annual and seasonal EV charging demand in 2018 and 2030. The seasonal charging demand ratio was calculated based on the total EV charging demand in 2018, whereas the seasonal charging demand for 2030 was predicted using the calculated ratio and the predicted annual EV charging demand.

As a result, EV charging frequency sampling data was used to predict EV charging demand during low, intermediate, and peak load times (Fig. 4) and the EV charging demand forecasting in 2030 (Table 4), extracted by considering the weights based on time. Table 5 summarizes the predicted EV charging demand in 2030, calculated by applying the proposed EV charging demand prediction algorithm.

The annual and seasonal EV charging demand in 2030 was predicted using the measured data of EV charging in 2018, the number of EVs, and the estimated number of EVs in 2030. Furthermore, the predicted EV charging demand in 2030 based on the grid load time classification was

TABLE 6. Results of monthly wind power output prediction error (MAE).

Month	Bus A	Bus B	Bus C	Bus D
3	11.43	10.94	6.64	13.19
4	15.65	15.17	7.89	17.94
5	9.89	12.53	6.38	12.62
6	8.65	6.85	3.68	6.19
7	**5.64**	7.36	**3.40**	**5.65**
8	8.12	8.12	5.31	9.47
9	10.29	10.32	5.71	11.40
10	8.95	7.16	7.87	11.31
11	10.32	**5.79**	8.63	14.69
12	14.16	12.15	10.11	14.43

TABLE 7. Wind power capacity factor (MW).

Time	Bus Name	Spring/Fall	Summer	Winter
Low load	A	20.15	12.57	22.79
	B	3.22	2.16	4.07
	C	83.66	51.14	108.45
	D	55.67	23.80	73.42
Intermediate load	A	19.68	11.74	23.01
	B	2.19	1.27	2.93
	C	81.15	47.09	108.63
	D	54.72	21.38	71.51
Peak load	A	20.46	12.52	22.56
	B	2.49	1.59	2.76
	C	92.39	58.88	102.51
	D	55.82	22.00	71.25

TABLE 8. New wind farm information.

Name	Installation capacity (MW)	Mapping Bus
Wind Farm A	25.2	BUS C
Wind Farm B	100	BUS D
Wind Farm C	100	BUS D
Wind Farm D	135	BUS C
Wind Farm E	125	BUS A
Wind Farm F	21	BUS A
Wind Farm G	20	BUS B
Wind Farm H	3	BUS B
Wind Farm I	20	BUS D

estimated using the sampling data of the charging frequency in time. These are used as input data for the system analysis in Section 4.

III. WIND POWER OUTPUT FORECASTING

In this section, an autoregressive integrated moving average with exogenous variables (ARIMAX) model is applied to predict the wind power output. The power grid was divided into four groups to predict the hourly wind power output based on the ARIMAX model. Additionally, the 154 kV bus in each group was designated as the representative bus of the corresponding defense.

TABLE 9. Pseudocode of decentralization of electric vehicle charging demand.

Algorithm 1. Decentralization of EVs charging demand

Input: EV charging data, Wind power data
Output: Line sensitivity of N-1 contingency (ACO)
Initialization: N=1,000 (Number of Sampling)

Step 1. EV charging demand prediction
1) Calculate weight (ω_h) of EV charging frequency for each time
2) Random sampling
for h = 1 to 24
$h_{freq} = N \times \omega_h$
3) Calculate $EV\ charging\ demand_{2030}$
$EV\ charging\ demand_{2018} \times \frac{The\ number\ of\ EV_{2030}}{The\ number\ of\ EV_{2018}}$
Step 2. Wind power output prediction
1) Correlation analysis
if correlation > 0.7
Select meteorological variables
2) ARIMAX model selection
$y_t = \sum_{i=1}^{p} \phi_i y_{t-i} + \sum_{j=1}^{q} \theta_j \varepsilon_{t-j} + \alpha x_t$
3) Prediction wind power output (P)
if P < 0 **then**
Return P = 0
if P > Installed Capacity **then**
Return P= Installed Capacity
Step 3. Power system analysis
if EV charging demand > Wind power output (predicted)
1) Select of system analysis scenario
2) System analysis (N-1 contingency)
3) Calculate Line sensitivity (ACO)
End

A. ENHANCED ARIMAX MODEL

The ARIMAX model is a multivariate time series prediction model incorporating external variables in a linear regression model based on the existing AIRMA model. Unlike the ARIMA model, which considers only one variable, the ARIMAX model predicts using multiple variables [19], [20]. Therefore, in this study, both the historical wind power output data and the measured wind speed, which had a high correlation with the wind power output, were considered as input data to predict wind power output using the improved ARIMAX model. Fig. 5 depicts the enhanced ARIMAX model algorithm.

Equation (2) represents the ARIMAX model equation. The first and second terms on the right-hand side of the equation denote the auto-regressive (AR) and moving average (MA) components, respectively.

$$y_t = \sum_{i=1}^{p} \phi_i y_{t-i} + \sum_{j=1}^{q} \theta_j \varepsilon_{t-j} + \alpha x_t, \tag{2}$$

where, ϕ_t, y_{t-i}, θ_q, ε_{t-j}, α, and x_t represent the coefficient of y_{t-i}, output lagged by time step i, coefficient of ε_{t-j}, white noise, coefficient of x_t, wind speed at time t.

The ARIMAX prediction model performs data preprocessing using the difference and transformation techniques as the stationarity verification of the input data necessitates normalization. The input variables used in the ARIMAX model comprises both endogenous and exogenous variables.

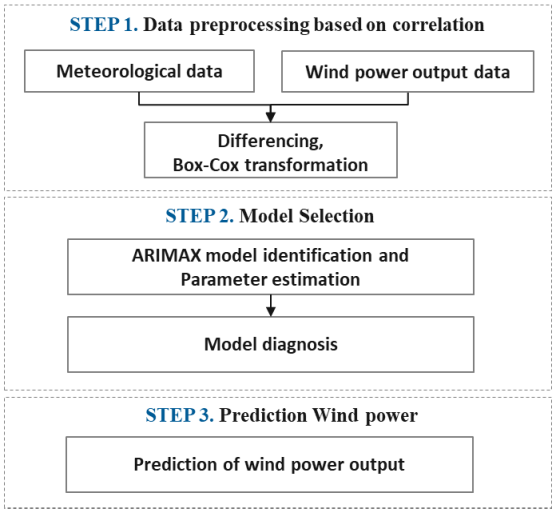

FIGURE 5. The enhanced ARIMAX model algorithm.

In this study, the measured data of past wind power output and the wind speed constitute the endogenous and exogenous variables, respectively. Furthermore, a suitable ARIMAX model must be selected based on the input data. Therefore, Akaike information criterion (AIC) statistics and residuals were calculated to verify the significance of the selected model. The wind power output was predicted using the enhanced ARIMAX model selected based on the ARIMAX model establishment, verification process, and the weather forecast data during the prediction period. Sections 3.B and 3.C describe the prediction method in detail.

B. COMPARISON OF WIND POWER OUTPUT AND WIND SPEED PATTERN

To predict the wind power output based on the ARIMAX model, it is necessary to analyze the wind power output and the measured wind speed data for each bus. In this study, the data correlation was analyzed using wind power and wind speed data collected from January 1 to December 31, 2018. Furthermore, the nearest distance was determined based on the distances calculated between each of the four 154-kV representative buses and each wind turbine.

The obtained wind power generation output data for each bus were grouped by mapping the wind turbine data to the located bus. Fig. 6 illustrates the comparison pattern of the wind power output and wind speed data in January 2018. It was confirmed that fluctuation patterns between the wind power output and wind speed data were similar for each bus. This implies that high correlation was observed between the wind power output and wind speed data. Therefore, the data of wind speed forecast, past wind power output, and wind speed can be used as input data for wind power output prediction.

C. PERFORMANCE OF WIND POWER OUTPUT FORECASITNG

In this section, the wind power output is predicted for each bus using the ARIMAX prediction model. Hourly wind power

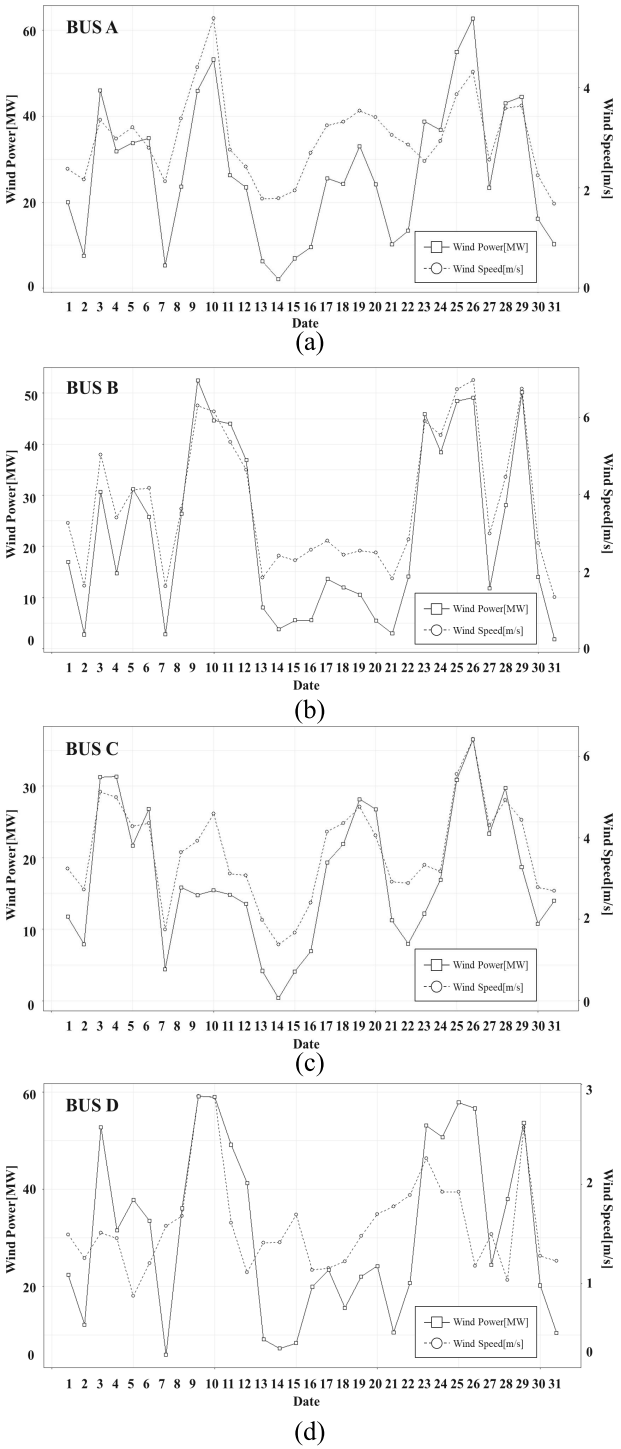

FIGURE 6. Comparison of wind power output and wind speed in January 2018.

output and wind speed data from January 1 to December 31, 2018 were used as input data for the prediction. The data of the previous 28 days from the time of prediction were set as the model training data, whereas the hourly wind power output and wind speed data from January 1 to February 28, 2018, were used as the ARIMAX model verification data. The wind power output prediction was performed hourly from March 1 to December 31, 2018. Fig. 7 illustrates the wind

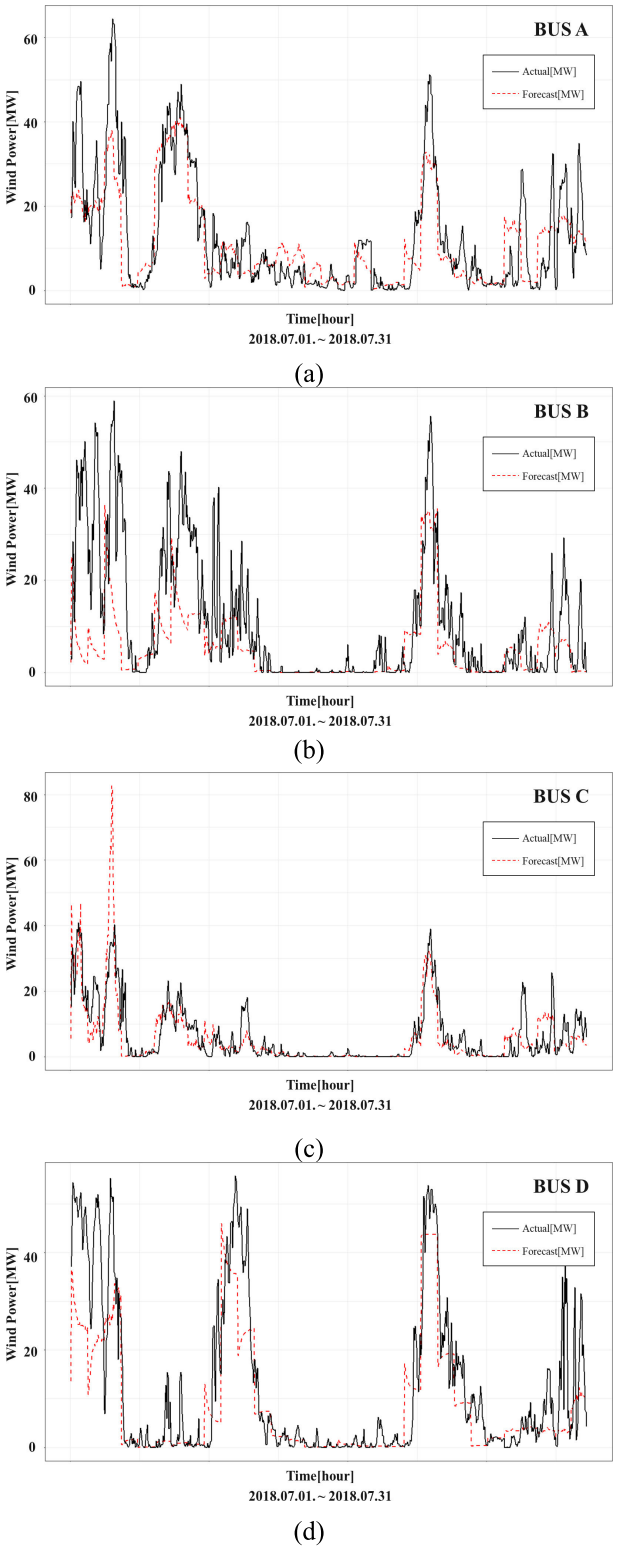

FIGURE 7. Comparison of wind power output forecasting with the measured power outputs in July 2018.

power from July 1 to July 31, 2018, as predicted by the model; the figure compares the predicted power outputs with the measured ones. The black line on the graph represents the actual wind power outputs, and the red dotted line represents

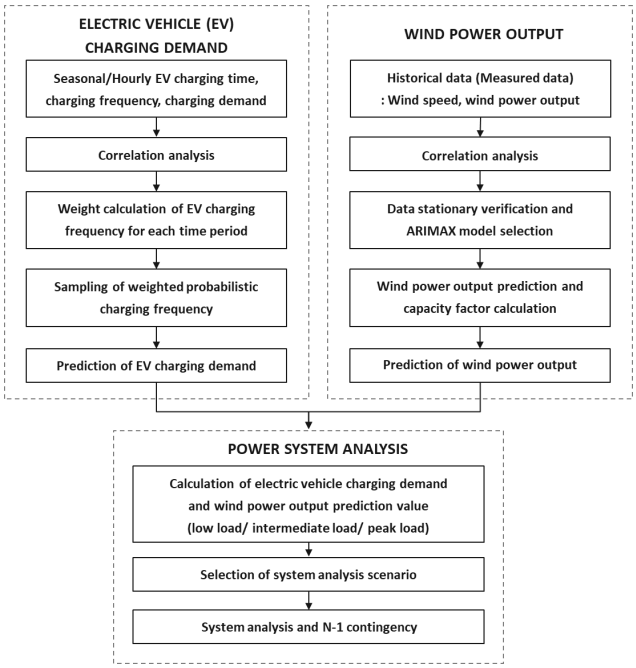

FIGURE 8. Proposed algorithm for decentralization of electric vehicle (EV) charging demand.

the predicted data. As a result of comparing the actual and predicted data, it was analyzed that the prediction was performed well with similar output patterns between the data.

To evaluate the predicted accuracy of wind power output for each bus, the mean absolute error (MAE) was used as an error evaluation index. The MAE function equation is

$$MAE = \frac{1}{N}\sum_{t=1}^{N}|Actual\ Output_t - Forecast\ Output_t| \quad (3)$$

The MAE of the monthly wind power output prediction of buses A–D was calculated using (3), and the obtained data are presented in Table 6. Based on the prediction error analysis, it was determined that the MAE of buses A–D in the prediction period were 20 or lower. Additionally, it confirmed that the ideal wind power output prediction was observed in July, owing to the lowest monthly average MAE.

The capacity factor of the wind power output for each bus was calculated based on the grid load time classification using the predicted wind power outputs. Table 7 summarizes the capacity factor details calculated using (4).

$$Capacity\ Factor\ [\%] = \frac{Actual\ Power}{Installed\ Capacity} \times 100 \quad (4)$$

Overall, nine new wind farms with a total installation capacity of 549.2 MW are planned to be built on Jeju Island by 2030 [21]. Table 8 presents the estimated installation capacities (MW) and names for each wind farm. These wind farms were mapped to the nearest bus based on the distance calculated from the previously selected four buses, A–D.

The estimated wind power output of the new wind farm that will penetrate the grid in 2030 is calculated using the

installation capacity provided and the capacity factor calculated for each bus.

IV. PROPOSED METHODOLOGY FOR SECURITY ANALYSIS

This section presents the system analysis performed by applying the EV charging demand predicted using probabilistic random sampling to the practical Jeju system. In this paper, six scenarios were selected for EV charging demand and wind power output prediction. Scenarios are constructed considering the load times (low load, intermediate load, peak load) and season (spring/fall, summer, winter). Fig. 8 depicts the proposed algorithm for decentralizing the EV charging demand.

The algorithm is performed in three steps, and details of each step are as follows:

- *Step 1:* EV charging demand prediction
  Seasonal and hourly charging frequency is analyzed using EV charging data. The parameters required to predict EV charging demand are EV charging start and end times, charging time, charging frequency, and charging power. The analyzed charging frequency is used as a weight for random sampling of EV charging demand prediction data for each time.
- *Step 2:* Wind power output prediction
  Wind power output prediction is performed using ARIMAX which is a multivariate time series prediction model. The parameters required for prediction are measured data (wind power output, wind speed) and wind speed prediction data.
- *Step 3:* Power system analysis
  Jeju power system analysis (50 bus) is performed using the data predicted through the Step 1 and 2 algorithms. Steady-state and N − 1 contingency are performed for each scenario, and sensitivity analysis is performed using aggregate contingency overload (ACO) [22], [23] for the branch flow (%) of N − 1 contingency.
  Table 9 shows the decentralization of EV charging demand proposed in this paper as a pseudocode. The prediction scenario (EV charging demand and wind power) created through the proposed algorithm was used to analyze the security of power system. This can be applied to establish a plan for decentralization of charging according to an increase in EV charging demand in the future.

The analysis was performed considering the weight of the charging frequency for each season and the wind power output forecasting using the enhanced arimax model. Table 10 summarizes the EV charging demand and wind power output prediction results discussed in sections 2 and 3.

The system analysis was performed considering two scenarios, namely the intermediate load and peak load times in summer, during which the EV charging demand is expected to be higher than the predicted wind power outputs.

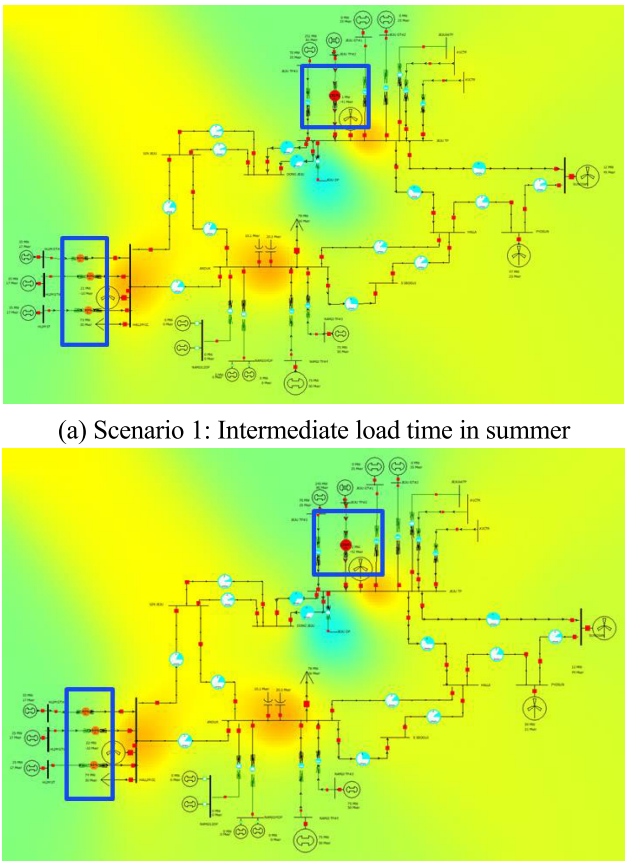

(a) Scenario 1: Intermediate load time in summer

(b) Scenario 2: Peak load time in summer

FIGURE 9. Results of power system analysis for each scenario.

Fig. 9 depicts the results of the Jeju system analysis for each scenario. The blue boxes in the figure indicate the bus in which the line overload occurred or the risk of overload was identified.

Table 11 shows the branch flow in which overload occurred as a result of N-1 contingency analysis.

Based on the system analysis, over 125% of overload was observed in Line B in both the scenarios and the line load rate of Line D was approximately 93%. Additionally, the N − 1 contingency performed at each of the two scenarios resulted in the line overload of Line B at all assumed failures. The cause of the overload was primarily analyzed considering two factors, namely the concentration of EV demand on Line B and nearby buses, and the increase in the power generation output due to the slack generator of Line B to maintain the balance of supply and demand of the system. Table 12 shows the ACO of the line with overload as a result of N − 1 contingency. The ACO (ACO_i, (%), ACO_i^T(%), ACO_{jk}^L(%)) was calculated for sensitivity analysis, and the equation for each ACO is as follows.

$$ACO_i\,(\%) = \sum_{\substack{Overloaed\ branches \\ that\ contingency\ i}} (Overload\,(\%) - 100), \tag{5}$$

TABLE 10. Electric vehicle charging demand and wind power output prediction for 2030 in Jeju island.

Time/ Season	Predicted output	Spring/Fall (March–May, September–October)	Summer (June–August)	Winter (January–February, November–December)
Low load	EV charging demand	31.0 MW	30.4 MW	29.7 MW
	Wind power output	162.7 MW	89.7 MW	208.7 MW
Intermediate load	EV charging demand	113.8 MW	117.2 MW	142.8 MW
	Wind power output	157.7 MW	81.5 MW	206.1 MW
Peak load	EV charging demand	122.3 MW	119.6 MW	94.6 MW
	Wind power output	171.2 MW	95.0 MW	199.1 MW

TABLE 11. Result of overload line (N−1 contingency).

Contingency Events	Number of Violation	Branch Name	Branch Flow (%) Scenario 1	Branch Flow (%) Scenario 2
# 1	2	Line B	139.1	132.9
		Line D	125.9	125.0
# 2	2	Line B	139.1	132.9
		Line D	125.9	125
# 3	1	Line B	138.7	132.5
# 4	1	Line B	140.1	133.8
# 5	1	Line B	137.9	131.7
# 6	1	Line B	137.9	131.7
# 7	1	Line B	138	131.9
# 8	1	Line B	137.9	131.8
# 9	1	Line B	138.0	131.8
# 10	1	Line B	138.4	132.2
# 11	1	Line B	138.0	131.8
# 12	1	Line B	137.9	131.8

$$ACO_i^T\ (\%) = \sum_{\substack{Contingencies \\ that\ scenario}} ACO_i, \tag{6}$$

$$ACO_{jk}^L\ (\%) = \sum_{\substack{Contingencies\ that \\ overloaded\ branch\ jk}} (Overload\ (\%) - 100), \tag{7}$$

where, $ACO_i\ (\%)$ is the sum of overloaded branches that contingency i, and $ACO_i^T\ (\%)$ is the sum of $ACO_i\ (\%)$ according to the scenario. $ACO_{jk}^L\ (\%)$ represent the aggregate contingency overload of branch jk.

As a result of the sensitivity analysis, the $ACO_I^T(\%)$ of the summer intermediate load scenario was calculated as the largest, which means that the system becomes the most vulnerable in the scenario. Since the most overload occurred in Line B, if electric vehicle charging demand and wind power output increase, it is necessary to temporarily shut down the operation of the EV charging station near the Line B, where the overload is expected to occur, to perform charging decentralization or reinforce the network. In this paper, two representative scenarios in which supply and demand imbalance occurred in the power system were selected and the effects of EVs and wind power generation on the power system were analyzed. If the EV charging demand modeling and wind power outputs prediction for 8760 hours as future work is performed, the system for more scenarios can be analyzed and the penetration level for optimal charging can be derived. Based on this, a method for decentralizing EV charging for a stable power system operation plan will be proposed.

TABLE 12. Line sensitivity analysis (N − 1 contingency).

Scenario	Contingency Events	Line B	Line D	$ACO_i(\%)$	$ACO_i^T(\%)$
Summer – Intermediate load	# 1	39.1	25.9	65.0	588.6
	# 2	39.1	25.9	65.0	
	# 3	38.7	0	38.7	
	⋮	⋮	⋮	⋮	
	# 14	37.9	0	37.9	
Summer – Peak load	# 1	32.9	25	57.9	500.5
	# 2	32.9	25	57.9	
	# 3	32.5	0	32.5	
	⋮	⋮	⋮	⋮	
	# 14	31.8	0	31.8	
$ACO_{jk}^L(\%)$		987.3	101.8	-	-

V. CONCLUSION

With several countries exploring the development of renewable energy source-based power generation, the resulting uncertainty in power demand and supply can significantly unbalance the power supply and demand. Furthermore, the increasing rise of EVs in the transportation sector generates variability in the power demand and power generation output, due to the increased charging demand and wind power installation capacity, respectively. To address the system uncertainty that may occur in future power systems, the prediction model to decentralize the EV charging demand is needed.

In this paper, the practical methodology for security analysis of grid-connected electric vehicle charging station with wind generating resources was proposed. The proposed algorithm is based on the EV charging demand prediction using probabilistic random sampling considering the weight of the charging frequency for each season. Additionally, wind power outputs were predicted using the enhanced ARIMAX model. The proposed model was applied to practical power system on Jeju Island, Korea. The results obtained verified that the proposed algorithm can help the establishment of an EV charging distribution plan. The proposed methodology will effectively solve the problems of imbalance between power supply and demand and power system uncertainty that

may occur due to the enhanced penetration rate of wind power facilities and EVs. The proposed algorithm has a limitation in that the prediction accuracy depends on the wind speed. Wind power output is predicted by using wind power outputs as endogenous variables and wind speed as and exogenous variables through the ARIMAX model. The reason for choosing wind speed as an exogenous variable is that the correlation coefficient with wind power outputs is high. However, if there is little correlation between wind speed and wind power outputs in some periods, the prediction accuracy can drop sharply. In addition, it is difficult to perform prediction when wind speed data for the forecast period, wind speed and wind outputs for the training period are omitted. In order to improve these limitations and increase the accuracy of wind power output prediction, as a future work, weather data such as wind speed of the target point will be predicted based on spatial modeling, and missing data pre-processing will be performed.

REFERENCES

[1] M. Bongiorno and T. Thiringer, "A generic DFIG model for voltage dip ride-through analysis," *IEEE Trans. Energy Convers.*, vol. 28, no. 1, pp. 76–85, Mar. 2013.
[2] N. Vidadili, E. Suleymanov, C. Bulut, and C. Mahmudlu, "Transition to renewable energy and sustainable energy development in azerbaijan," *Renew. Sustain. Energy Rev.*, vol. 80, pp. 1153–1161, Dec. 2017.
[3] Y. A. Kaplan, "Overview of wind energy in the world and assessment of current wind energy policies in turkey," *Renew. Sustain. Energy Rev.*, vol. 43, pp. 562–568, Mar. 2015.
[4] M. Alves, R. Segurado, and M. Costa, "On the road to 100% renewable energy systems in isolated islands," *Energy*, vol. 198, May 2020, Art. no. 117321, doi: 10.1016/j.energy.2020.117321.
[5] IEA. *Global EV Outlook 2020*. Accessed: Apr. 11, 2021. [Online]. Available: https://www.iea.org/reports/global-ev-outlook-2020
[6] Korea Ministry of Land, Infrastructure and Transport (MOLIT). *Korean Version of the Green New Deal*. Accessed: Apr. 11, 2021. [Online]. Available: http://www.molit.go.kr/newdeal/sub/sub_1_1.jsp
[7] H. S. Sims *et al.*, "Direction of the Korean version of the Green New Deal: Diagnosis and suggestions," Korea Energy Econ. Inst., 2020, vol. 1.
[8] Korea Ministry of Trade. *Renewable Energy 3020 Implementation Plan*. [Online]. Available: https://www.motie.go.kr/motie/py/brf/motiebriefing/motiebriefing404.do
[9] Jeju Special Self-Governing Province. *Carbon-Free Island (CFI) Jeju by 2030*. Accessed: Apr. 11, 2021. [Online]. Available: https://www.jeju.go.kr/cfi/index.htm
[10] J. Dai, M. Dong, R. Ye, A. Ma, and W. Yang, "A review on electric vehicles and renewable energy synergies in smart grid," in *Proc. China Int. Conf. Electr. Distrib. (CICED)*, Aug. 2016, pp. 1–4.
[11] S. Iqbal, A. Xin, M. U. Jan, M. A. Abdelbaky, H. U. Rehman, S. Salman, S. A. A. Rizvi, and M. Aurangzeb, "Aggregation of EVs for primary frequency control of an industrial microgrid by implementing grid regulation & charger controller," *IEEE Access*, vol. 8, pp. 141977–141989, 2020.
[12] L. Yazdi, R. Ahadi, and B. Rezaee, "Optimal electric vehicle charging station placing with integration of renewable energy," in *Proc. 15th Iran Int. Ind. Eng. Conf. (IIIEC)*, Jan. 2019, pp. 47–51.
[13] O. Avatefipour, A. S. Al-Sumaiti, A. M. El-Sherbeeny, E. M. Awwad, M. A. Elmeligy, M. A. Mohamed, and H. Malik, "An intelligent secured framework for cyberattack detection in electric Vehicles' CAN bus using machine learning," *IEEE Access*, vol. 7, pp. 127580–127592, 2019.
[14] X. Gong, F. Dong, M. A. Mohamed, O. M. Abdalla, and Z. M. Ali, "A secured energy management architecture for smart hybrid microgrids considering PEM-fuel cell and electric vehicles," *IEEE Access*, vol. 8, pp. 47807–47823, 2020.
[15] H. Mehrjerdi and R. Hemmati, "Stochastic model for electric vehicle charging station integrated with wind energy," *Sustain. Energy Technol. Assessments*, vol. 37, Feb. 2020, Art. no. 100577.
[16] E. Taibi, C. Fernández del Valle, and M. Howells, "Strategies for solar and wind integration by leveraging flexibility from electric vehicles: The barbados case study," *Energy*, vol. 164, pp. 65–78, Dec. 2018.
[17] Korea Electric Power Corporation (KEPCO). *Grid Load Time Classification*. Accessed: Apr. 11, 2021. [Online]. Available: http://cyber.kepco.co.kr/ckepco/front/jsp/CY/D/C/CYDCHP00403.jsp
[18] *Jeju Special Self-Governing Province*. Accessed: Apr. 11, 2021. [Online]. Available: https://www.jeju.go.kr/pub/skin/skin_20.09.0/doc.html?fn=1e4b34cd-0066-4007-9b0d-16b654d79575.hwp&rs=/files/convert2020/201905
[19] Q. Xu, W. Li, D. Kong, X. Zhao, X. Wang, Y. Li, Y. Shen, X. Wang, and Z. Zhao, "Ultra-short-term wind speed forecast based on WD-ARIMAX-GARCH model," in *Proc. IEEE 2nd Int. Conf. Autom., Electron. Electr. Eng. (AUTEEE)*, Nov. 2019, pp. 219–222.
[20] D. Peter and P. Silvia, "ARIMA vs. ARIMAX–which approach is better to analyze and forecast macroeconomic time series," in *Proc. 30th Int. Conf. Math. Methods Econ.*, vol. 2, Sep. 2012, pp. 136–140.
[21] Jeju Special Self-Governing Province. *Jeju Wind Power Status*. Accessed: Apr. 11, 2021. [Online]. Available: https://www.jeju.go.kr/pub/skin/skin_20.09.0/doc.html?fn=8ba653e1-6f23-4fff-96fa-b07b0e3bbe65.hwp&rs=/files/convert2020/202005/
[22] S. Grijalva and A. M. Visnesky, "The effect of generation on network security: Spatial representation, metrics, and policy," *IEEE Trans. Power Syst.*, vol. 21, no. 3, pp. 1388–1395, Aug. 2006.
[23] S. Grijalva, S. R. Dahman, K. J. Patten, and A. M. Visnesky, "Large-scale integration of wind generation including network temporal security analysis," *IEEE Trans. Energy Convers.*, vol. 22, no. 1, pp. 181–188, Mar. 2007.

GYEONGMIN KIM (Student Member, IEEE) received the B.S. degree in electrical engineering from Sangmyung University, South Korea, in 2020. She is currently pursuing the degree with the Department of Climate and Energy Systems Engineering, Ewha Womans University. Her research interest includes probabilistic estimation of renewable energy resources for power grid.

JIN HUR (Senior Member, IEEE) received the B.S. and M.S. degrees in electrical engineering from Korea University, Seoul, South Korea, in 1997 and 1999, respectively, and the Ph.D. degree in electrical and computer engineering from The University of Texas at Austin, in 2012. He is currently an Associate Professor with the Department of Climate and Energy Systems Engineering, Ewha Womans University. His research interest includes integrate high-level of variable generating resources into electric power systems.